

Generalized Lotka-Volterra Systems with Time Correlated Stochastic Interactions

Samir Suweis^{1,2,3}, Francesco Ferraro^{1,2,4}, Christian Grilletta¹, Sandro Azaele^{1,2,4,*} and Amos Maritan^{1,2,4,*}

¹*Laboratory of Interdisciplinary Physics, Department of Physics and Astronomy “G. Galilei”,
University of Padova, Padova, Italy*

²*INFN, Sezione di Padova, via Marzolo 8, Padova 35131, Italy*

³*Padova Neuroscience Center, University of Padova, Padova, Italy*

⁴*National Biodiversity Future Center, Piazza Marina 61, 90133 Palermo, Italy*



(Received 28 July 2023; revised 19 February 2024; accepted 30 August 2024; published 16 October 2024)

In this Letter, we explore the dynamics of species abundances within ecological communities using the generalized Lotka-Volterra (GLV) model. At variance with previous approaches, we present an analysis of GLV dynamics with temporal stochastic fluctuations in interaction strengths between species. We develop a dynamical mean field theory (DMFT) tailored for scenarios with colored noise interactions, which we term annealed disorder, and simple functional responses. Our DMFT framework enables us to show that annealed disorder acts as an effective environmental noise; i.e., every species experiences a time-dependent environment shaped by the collective presence of all other species. We then derive analytical predictions for the species abundance distribution that well match empirical observations. Our results suggest that annealed disorder in interaction strengths favors species coexistence and leads to a large pool of very rare species in the systems, supporting the insurance theory of biodiversity. This Letter offers new insights not only into the modeling of large ecosystem dynamics but also proposes novel methodologies for examining ecological systems.

DOI: [10.1103/PhysRevLett.133.167101](https://doi.org/10.1103/PhysRevLett.133.167101)

Understanding the mechanisms driving the biodiversity patterns observed across various ecosystems has long been a central challenge in community ecology [1,2]. Traditionally, ecologists believed that more complex ecosystems, containing a greater number of species and interactions, should exhibit greater stability [3]. This notion was fundamentally challenged by May, who introduced the concept of stability bound for randomly assembled ecosystems [4], showing that the larger the number of interactions and their variability, the less stable the system is. This result is known as “diversity-stability paradox” [5]. One key area of research that has gained momentum since May’s pivotal work focuses on understanding the role of interaction networks on the stability and species coexistence within large communities [2,6–10]. Given the inherent unknowns in species interactions, several recent works have proposed modeling the dynamics of interacting species through generalized Lotka-Volterra (GLV) equations with quenched random disorder (QGLV), where the underlying interaction network is fully connected, leading to a number of interesting results [11–15]. The phase diagram of these models is essentially divided into three regions of qualitatively different behaviors: a system may converge to a fixed point, reach a multiple-attractors state, or have populations which grow indefinitely [13,14,16]. Furthermore, the addition of

demographic noise to the QGLV leads to new phases such as a Gardner phase [17].

The QGLV model assumes that species interactions remain constant over time. However, empirical ecological systems are characterized by temporal fluctuations in species interactions, influenced by variations in environmental conditions, resource availability, and other factors that operate on a timescale comparable to population dynamics [18–22]. In the single fixed point phase, the stability of the QGLV model decreases as the fraction of nonzero interactions and the heterogeneity of the interaction strengths increases [13,23]. In particular, such ecological communities dynamically mitigate instability by reducing species diversity, eventually achieving a marginally stable state [13], consistent with previously obtained theoretical bounds [5]. Moreover, the distribution of the stationary populations within the ecological community (known as species abundance distribution, or SAD), as obtained in the unique equilibrium phase and in the limit of a large number of species within the dynamical mean field theory (DMFT), is a truncated Gaussian [14,16]. This distribution is very different from the heavy tail SAD observed in empirical microbial [24], plankton [25], or forest [26] communities.

In the present Letter, within the established framework of the GLV model featuring a fully connected random interaction network, we consider time-dependent species interactions and a Monod functional response, commonly used for modeling the growth of microorganisms [27].

*These authors contributed equally to the work.

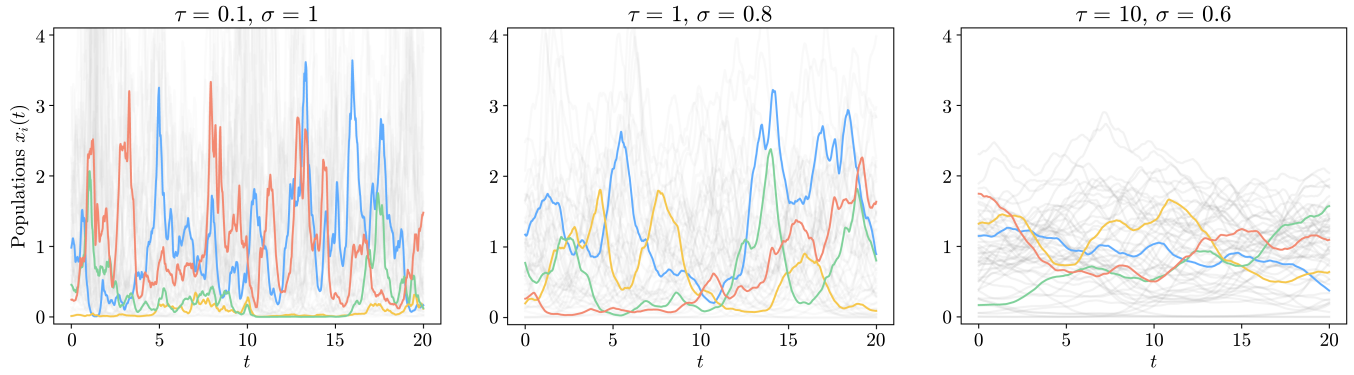


FIG. 1. Examples of species abundances trajectories obtained by simulating Eq. (1) for $S = 100$, $h = 0$, and different values of the characteristic correlation time τ and noise intensity σ . (a) $\tau = 0.1$, $\mu = 0$, $\sigma = 1$; (b) $\tau = 1$, $\mu = 0$, $\sigma = 0.8$; (c) $\tau = 10$, $\mu = 0$, $\sigma = 0.6$. Fluctuating behavior is instrumental in promoting the coexistence of multiple species within the ecosystem and is present for all ranges of τ , including the limit $\tau \rightarrow 0$. Different values of σ as τ varies are chosen to better visualize population fluctuations as a function of time.

Specifically, we adopt the hypothesis that any interaction between an arbitrary pair of species can be modeled as stochastic colored noise, which we call annealed GLV (AGLV). The introduction of temporal stochastic fluctuations in the strengths of species interactions yields results that fill some of the aforementioned gaps for the QGLV. In fact, unlike previous models where environmental noise was introduced externally with predefined statistical properties [24,28], our model incorporates an effective random environment whose characteristics are determined self-consistently. In this way, every species experiences an environment shaped by the collective presence of all other species. We find that temporal fluctuations in the species interactions promote species diversity and generate SAD that aligns with data, where the majority of species are rare, and most individuals belong to a small fraction of all species [29].

Let us consider $x_i(t)$, the population density at time t of the species i . Then the dynamics of the AGLV system with colored noise for S interacting species are given by

$$\dot{x}_i(t) = x_i(t) \left[r_i(1 - x_i(t)/K_i) + \sum_{j \neq i} \alpha_{ij}(t) J[x_j(t)] + h_i(t) \right], \quad (1)$$

with $i = 1, \dots, S$, and where $\alpha_{ij}(t) = \mu/S + \sigma z_{ij}(t)/\sqrt{S}$ for $i \neq j$ and $\{z_{ij}(t) : t > 0\}$ are independent Gaussian random variables with $\overline{z_{ij}(t)} = 0$, $\overline{z_{ij}(t)z_{kl}(t')} = \delta_{i,k}\delta_{j,l}Q(\Delta t|\tau) = \delta_{i,k}\delta_{j,l}[(1 + 2\tau/\tau_0)/2\tau]e^{-\Delta t/\tau}$, where $\delta_{x,y}$ is the Kronecker δ , and $\Delta t = |t - t'|$. $J(x)$ is a generic function of x , and in particular we will consider two cases: $J(x) = x$, to make direct comparison with QGLV, and $J(x) = [x/(1 + cx)]$, where c is known as handling time [30]. $h_i(t)$ is a possible time-dependent external field. The amplitude of the noise $Q(\Delta t|\tau)$ is chosen so that in the

limit $\tau \rightarrow \infty$ we recover the case of quenched disorder. For simplicity, we set $\tau_0, r_i, K_i = 1$ for $i = 1, \dots, S$ and work with dimensionless variables and parameters. From this general annealed formulation with colored noise, the limit $\tau \rightarrow 0$ corresponds to annealed white-noise (AWN) dynamics. In Fig. 1 we show the effect of time correlated noise on the species abundance evolution for $J[x_j(t)] = x_j(t)$. In our model fluctuations scale like the size of the population, generating a time-dependent multiplicative noise that keeps the trajectories away from zero, thus preventing their extinction for any finite τ . This behavior is substantially different from the one of models with quenched noise, where all species' populations with a negative growth rate are doomed to extinction in the infinite time limit. Species populations undergo fluctuations between high and low abundances, with an average frequency which depends on the value of τ . This fluctuating behavior is instrumental in promoting the coexistence of multiple species within the ecosystem and is present for all ranges of finite τ , including the limit $\tau \rightarrow 0$. As we show, the same results hold for $J[x_j(t)] = \{x_j(t)/[1 + cx_j(t)]\}$. Facilitating species coexistence through fluctuations is a mechanism that has also been observed in the chaotic phase of the QGLV [15,31,32] or similar models [29], leading to a large pool of very rare species in the systems, supporting the insurance theory of biodiversity [26,29].

The DMFT for the general AGLV Eq. (1) is given by [see Sec. 1 in Supplemental Material (SM) [33]]

$$\dot{x}(t) = x(t)[1 - x(t) + \mu M(t) + \sigma \eta(t) + h(t)], \quad (2)$$

where $M(t) = E[x(t)]$, $E[\cdot]$ indicates the expected value, and in the following we set $h(t) = 0$. The self-consistent Gaussian noise $\eta(t)$ is such that $E[\eta(t)] = 0$ and $E[\eta(t)\eta(t')] = Q(\Delta t|\tau)E\{J[x(t)]J[x(t')]\}$.

From Fig. 5 in SM [33], we can see that at stationarity, the (connected) autocorrelation function of $J[x(t)]$ has an

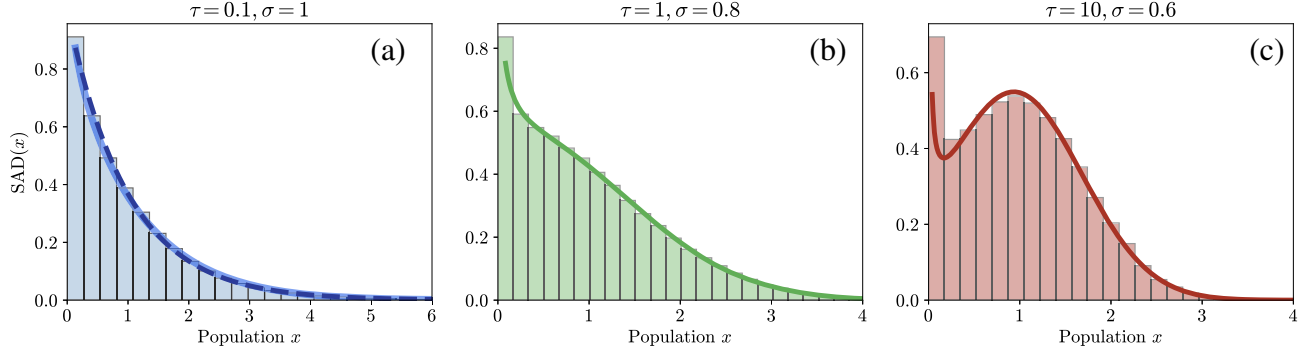


FIG. 2. Comparison between numerical and analytical solutions. The histograms represent the species abundance distributions (SADs) obtained by simulating the full AGLV system given by Eq. (1) for $S = 100$ species; the solid lines are the corresponding SADs given by the DMFT and UCNA. (a) Eq. (4) with $\tau = 0.1$. As a blue dashed line we also show the AWN solution given by Eq. (5). (b),(c) Colored noise AGLV [Eq. (4)] with $\tau = 1$ and $\tau = 10$, respectively. The analytical DMFT perfectly describes the SAD given by the numerical simulations of the full system. The initial conditions of the populations in all cases are drawn from $x_i \sim U[0.1, 0.2]$, where U denotes the uniform distribution, while the values μ and σ are as in Fig. 1. The different values of σ as τ varies and were chosen to better visualize the change of the SAD toward that of a truncated Gaussian plus a Dirac δ at $x = 0$ obtainable in the $\tau = +\infty$ limit. See supplemental figures (Sec. 3 of SM [33]) for other values of μ , σ , and τ .

exponentiallike decay:

$$\mathbb{E}\{J[x(t)]J[x(t')]\} - \mathbb{E}^2[J(x)] \approx \{\mathbb{E}[J(x)^2] - \mathbb{E}^2[J(x)]\}e^{-\frac{|t-t'|}{\tau_x}}, \quad (3)$$

and exploiting Eq. (3) we can simplify the self-consistency for η as $\mathbb{E}[\eta(t)\eta(t')] = Q(\Delta t|\bar{\tau})\mathbb{E}[J(x)^2]$, at least in the relevant regime $|\Delta t| = |t - t'| \ll \tau_x$ in which the connected autocorrelation function can be approximated by the non-connected autocorrelation function, with the new effective timescale $\bar{\tau} = 1/[1/\tau + (1 - \mathbb{E}^2[J(x)]/\mathbb{E}[J(x)^2])/\tau_x]$. (see Sec. 2 in SM [33] for further details).

With this simplification we can now use the unified colored noise approximation (UCNA) [34,35] on Eq. (2), which, for both cases of $J(x)$ considered here, leads to the same stationary SAD:

$$P_\tau^*(x) = \frac{x^{-1+\delta_\tau}}{Z(\delta_\tau, D, \bar{\tau})} \left(\frac{1}{\bar{\tau}} + x \right) e^{-\frac{x}{\bar{\tau}} - \frac{\bar{\tau}}{2D}(x-\bar{x})^2}, \quad (4)$$

where $x > 0$, $Z(\delta_\tau, D, \bar{\tau})$ is the normalization constant, that can be computed analytically, $\delta_\tau = (1 + \mu M^*)/D(\tau)$, $D(\tau) = \sigma^2 \mathbb{E}^*[J(x)^2](1 + 2\tau)\bar{\tau}(\tau)/2\tau$, and $\bar{x} = 1 + \mu M^*$ [$\mathbb{E}^*(\cdot)$ denotes the average with the distribution P_τ^* and $M^* = \mathbb{E}^*[J(x)]$]. Notice that $P_\tau^*(x)$ is essentially an interpolation between a truncated Gaussian and a Gamma distribution. The former is known to be the solution for the SAD of the DMFT in the case of random quenched interactions in the single equilibrium phase [14,16], while the latter is shown below to be the exact solution of the AWN case, corresponding to the limit $\bar{\tau} \sim \tau \rightarrow 0$ of Eq. (2).

UCNA is recognized for its exactness in both $\tau = 0$ and $\tau = +\infty$, proving to be a reliable interpolation method for intermediate values of τ [34,35]. This is explicitly

illustrated in Fig. 2, where the analytical solution of the SADs for various τ values, obtained through both the DMFT and UCNA, is compared with numerical solutions derived from integrating Eq. (1) for a system comprising $S = 100$ species with $J(x) = x$. In Sec. 2.2 of SM [33], we show that the same result also holds for the case with the Monod functional response. We have also performed a sensitivity analysis, showing that the analytical solutions match the numerical ones very well for a wide range of parameters.

As demonstrated in both Figs. 1 and 2, the introduction of time-dependent fluctuations in interactions promotes species coexistence. This is attributed to the induced fluctuating behavior, causing the species' growth rate to transition from negative to positive, preventing extinctions, as also verified numerically (see Fig. 2). Only when $\tau = +\infty$ a Dirac's δ develops at $x = 0$, whose mass represents the fraction of extinct species. However, in practical applications, distinguishing rare species from extinct ones in samples with a finite number of species, S , requires consideration. This can be addressed by introducing a threshold value, x_{th} . As shown in Fig. 3, we find that the fraction of extinct species increases with τ . This finding indicates that rapid stochastic variability in species interactions promotes coexistence, while slow or static interactions are detrimental. Each point in Fig. 3 is given by $\int_0^{x_{th}} P_\tau^*(x) dx$ with $P_\tau^*(x)$ obtained as in Fig. 2. The horizontal dashed lines in Fig. 3 represent the number of extinct species in the quenched disorder limit [14,16]. In Sec. 2.3 of SM [33], we also show that this result holds for different values of the extinction threshold.

In the white-noise $\tau \rightarrow 0$ limit the DMFT equation is the same of Eq. (2), but in this case with $\mathbb{E}[\eta(t)\eta(t')] = \Sigma^2(t)\delta(t-t')$, $\Sigma^2(t) = \mathbb{E}\{J[x(t)]^2\}$, and the multiplicative noise term $x(t)\eta(t)$ should be interpreted in the

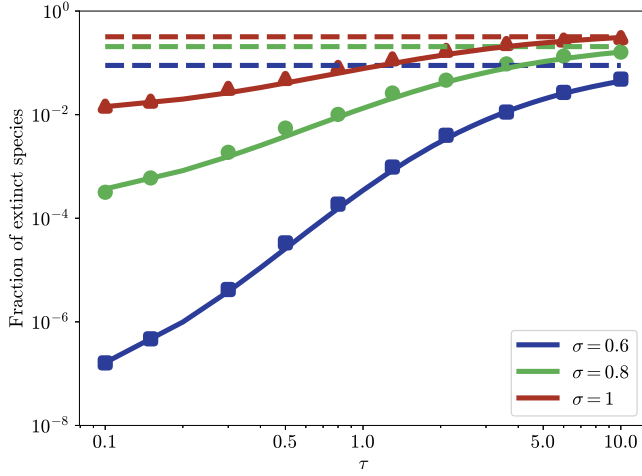


FIG. 3. Fraction of extinct species at stationarity for $\mu = 0$ and different values of interactions heterogeneity (given by σ) as a function of the characteristic time of species interaction fluctuations (τ). The solid lines are instead analytically obtained by assuming that $\tau_x \sim \tau$ (see Sec. 2.3 in SM [33] for further details), allowing a simple estimation of the fraction of extinct species without fitting the model parameters. Here the extinction threshold is set to $x_{th} = 10^{-2}$, but the qualitative behavior does not depend on the specific value of x_{th} . We refer to Sec. 23 in SM for all the details.

Stratonovich sense [36]. At stationarity, the self-consistency imposes $M^* = E^*[J(x)]$ and $\Sigma^{*2} = E^*[J(x)^2]$. The exact stationary distribution P_0^* can be derived from the Fokker-Planck equation corresponding to Eq. (2), and it reads [for any $J(x)$]:

$$P_0^*(x) = \frac{\beta^\delta}{\Gamma(\delta)} x^{-1+\delta} e^{-\beta x}, \quad (5)$$

and it coincides with the limits of $P_\tau^*(x)$ when $\tau \rightarrow 0$ as discussed in detail in the section “White-Noise Limit” in SM [33]. We also have $\lim_{\tau \rightarrow 0} \delta_\tau = 2(1 + \mu M^*)/(\sigma^2 \Sigma^{*1}) \equiv \delta$ with $M^* = 1/(1 - \mu)$ and $\Sigma^{*2} = \delta(\delta + 1)/\beta^2$ for $J(x) = x$. Similar results are obtained for the case with the functional response (see SM [33], Sec. 2.2).

For $J(x) = x$ we can write explicitly the SAD’s parameters as a function of μ and σ as (see Sec. 2.4 in SM [33])

$$\beta = \frac{\sigma^2}{2} \delta(\delta + 1); \quad \delta = \frac{2}{\sigma^2} (1 - \mu) - 1, \quad (6)$$

while for the case with functional response, we can simply solve numerically the equations for M^* and Σ^* as a function of β and δ .

The predicted SADs by Eq. (4) through the DMFT and UCNA are plotted as continuous lines in Fig. 2. The parameters are obtained by first fitting the autocorrelation, checking the agreement with the empirical parameters (error below 5%; see Sec. 2 in SM [33]). In panel

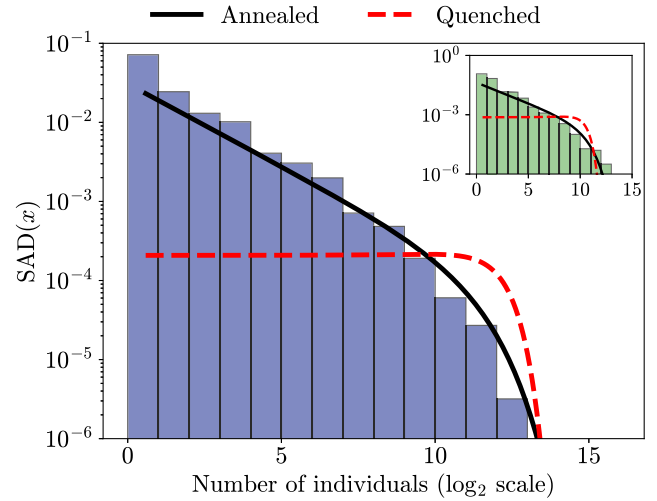


FIG. 4. Comparison with empirical data. The main panel shows the SAD in the Barro Colorado Island forest; the black line is the fit of the Gamma distribution predicted by AGLV, while the red dashed line is the fit of the Gaussian distribution predicted by QGLV. The parameters of the distribution have been estimated by using maximum likelihood. The inset shows the SAD in a Caribbean coral reef.

(a) we also plot, as a dark blue dashed line, the AWN solution $P_0^*(x)$ given by Eq. (5). In this case, the distribution parameters are directly calculated from Eq. (6) as a function of μ and σ .

To address the empirical relevance of our theoretical findings, we have analyzed two datasets: trees from a tropical forest [37] and coral reefs [38]. Figure 4 shows the SADs using Preston (log2) scale (as usually done in this context [1]). The empirical SADs were then compared with the truncated Gaussian and Gamma distributions that can be derived from the QGLV and AGLV, respectively. We find that the empirical SADs are accurately described by the AGLV model, while the QGLV model fails to reproduce these patterns. This comparison proves the empirical relevance of our model, demonstrating its applicability to real-world ecological data.

As is well-known in the literature, the QGLV model exhibits certain pathologies that lead to the existence of a region in the phase diagram where densities diverge [39]. These divergences also persist in the AGLV model. Actually, the temporal fluctuations in interactions expand the region of the phase space where the model does not converge (see Sec. 4 in SM [33] for further details). However, when the Monod functional response is introduced through a bounded $J(x)$, we prevent indefinite population growth, eliminating any divergences and dependencies on the initial conditions. Therefore, the phase diagram displays only the stable stationary state for any values of μ and σ . The stationary solution, Eq. (4), does not depend on the specific form of $J(x)$. The specific choice of $J(x)$ enters only through self-consistencies, i.e., $J(x)$

determines the random environment experienced by the species.

In this Letter, we have undertaken an investigation into the GLV equations with annealed disorder, incorporating finite correlation time and simple functional responses. We have determined the corresponding dynamical mean-field equations for a large number of species, which do not depend on the specific form of $J(x)$. The inclusion of temporal stochastic fluctuations in the strengths of species interactions has resulted in a diverse range of ecologically significant outcomes. First, the introduction of annealed disorder in the GLV equations, for any finite correlation time, has exerted a substantial positive influence on the biodiversity of the system. Specifically, when the dynamics of the system converges to the stationary distribution, we observe fluctuations in the dynamics of species populations, where species abundances alternate between high and low values, favoring the coexistence of all species and supporting the insurance theory of biodiversity [26,29]. This is, in fact, a similar outcome to what QGLV models found in the chaotic phase [15,32] when introducing an immigration rate λ , which explicitly prevents extinctions. Second, in the white-noise limit, the DMFT leads to the stochastic logistic model, a phenomenological model that proved to be consistent with several macroecological laws in microbial ecosystems [24,28]. In particular, the analytical species abundance distribution derived from the DMFT follows the Gamma distribution, a widely utilized probability distribution in macroecology [1,37]. Again, similar truncated fat-tailed distribution has recently been numerically found in the chaotic phase of the QGLV [32] and in the GLV with strong interactions [29,40,41] with immigration. Eventually, we have presented a refinement of the model, through the inclusion of a simple functional response. We have shown that it maintains not only the core phenomenology described above but also rectifies any nonphysical divergences observed in the classic QGLV and in the AGLV. Thus, it enhances the model's realism and applicability without sacrificing its fundamental characteristics and predictive capabilities. This work opens various avenues of research, including the integration of quenched and annealed disorder and the correlations between pairs of interacting species [14,16] or more complex hierarchical correlation structures [42]. More generally, the methodology presented here can be exploited to study the effect of annealed disorder also in other ecological dynamics. Moreover, to further improve the AGLV model, it would be valuable to explore sparse interaction networks instead of the fully connected ones examined here and in previous works [12–17] for the quenched version. However, unlocking the dynamics of this intriguing scenario requires a more comprehensive generalization of the DMFT approach [43]. The exploration of such directions holds significant promise for advancing the modeling of large-scale ecosystem dynamics,

understanding emergent macroecological patterns observed in empirical data, and investigating the influence of environmental fluctuations on species coexistence.

Acknowledgments—We wish to acknowledge Jacopo Grilli and Davide Bernardi for critical reading of the manuscript and useful discussions. F.F. thanks Matteo Guardiani and the Information Field Theory group at the Max-Planck Institute for Astrophysics for their hospitality and helpful comments. S.S. acknowledges financial support from the MUR - PNC (DD n. 1511 30-09-2022) Project No. PNC0000002, DigitAI lifelong pRevEntion (DARE). S.A., F.F., C.G., and A.M. also acknowledge the support by the Italian Ministry of University and Research (project funded by the European Union—Next Generation EU: PNRR Missione 4 Componente 2, “Dalla ricerca all’impresa,” Investimento 1.4, Progetto CN00000033).

-
- [1] S. Azaele, S. Suweis, J. Grilli, I. Volkov, J. R. Banavar, and A. Maritan, Statistical mechanics of ecological systems: Neutral theory and beyond, *Rev. Mod. Phys.* **88**, 035003 (2016).
 - [2] N. I. van den Berg, D. Machado, S. Santos, I. Rocha, J. Chacón, W. Harcombe, S. Mitri, and K. R. Patil, Ecological modelling approaches for predicting emergent properties in microbial communities, *Nat. Ecol. Evol.* **6**, 855 (2022).
 - [3] K. S. McCann, The diversity–stability debate, *Nature (London)* **405**, 228 (2000).
 - [4] R. M. May, Will a large complex system be stable?, *Nature (London)* **238**, 413 (1972).
 - [5] S. Allesina and S. Tang, The stability–complexity relationship at age 40: A random matrix perspective, *Popul. Ecol.* **57**, 63 (2015).
 - [6] S. Allesina and S. Tang, Stability criteria for complex ecosystems, *Nature (London)* **483**, 205 (2012).
 - [7] C. Tu, J. Grilli, F. Schuessler, and S. Suweis, Collapse of resilience patterns in generalized Lotka–Volterra dynamics and beyond, *Phys. Rev. E* **95**, 062307 (2017).
 - [8] Y. Xiao, M. T. Angulo, J. Friedman, M. K. Waldor, S. T. Weiss, and Y.-Y. Liu, Mapping the ecological networks of microbial communities, *Nat. Commun.* **8**, 2042 (2017).
 - [9] C. A. Serván, J. A. Capitán, J. Grilli, K. E. Morrison, and S. Allesina, Coexistence of many species in random ecosystems, *Nat. Ecol. Evol.* **2**, 1237 (2018).
 - [10] D. Gupta, S. Garlaschi, S. Suweis, S. Azaele, and A. Maritan, Effective resource competition model for species coexistence, *Phys. Rev. Lett.* **127**, 208101 (2021).
 - [11] D. A. Kessler and N. M. Shnerb, Generalized model of island biodiversity, *Phys. Rev. E* **91**, 042705 (2015).
 - [12] M. Barbier, J.-F. Arnoldi, G. Bunin, and M. Loreau, Generic assembly patterns in complex ecological communities, *Proc. Natl. Acad. Sci. U.S.A.* **115**, 2156 (2018).
 - [13] G. Biroli, G. Bunin, and C. Cammarota, Marginally stable equilibria in critical ecosystems, *New J. Phys.* **20**, 083051 (2018).

- [14] T. Galla, Dynamically evolved community size and stability of random Lotka-Volterra ecosystems (a), *Europhys. Lett.* **123**, 48004 (2018).
- [15] M. T. Pearce, A. Agarwala, and D. S. Fisher, Stabilization of extensive fine-scale diversity by ecologically driven spatio-temporal chaos, *Proc. Natl. Acad. Sci. U.S.A.* **117**, 14572 (2020).
- [16] G. Bunin, Ecological communities with Lotka-Volterra dynamics, *Phys. Rev. E* **95**, 042414 (2017).
- [17] A. Altieri, F. Roy, C. Cammarota, and G. Biroli, Properties of equilibria and glassy phases of the random Lotka-Volterra model with demographic noise, *Phys. Rev. Lett.* **126**, 258301 (2021).
- [18] J.N. Thompson, The evolution of species interactions, *Science* **284**, 2116 (1999).
- [19] S. Suweis, F. Simini, J.R. Banavar, and A. Maritan, Emergence of structural and dynamical properties of ecological mutualistic networks, *Nature (London)* **500**, 449 (2013).
- [20] F. Fiegna, A. Moreno-Letelier, T. Bell, and T.G. Barraclough, Evolution of species interactions determines microbial community productivity in new environments, *ISME J.* **9**, 1235 (2015).
- [21] M. Ushio, C.-h. Hsieh, R. Masuda, E.R. Deyle, H. Ye, C.-W. Chang, G. Sugihara, and M. Kondoh, Fluctuating interaction network and time-varying stability of a natural fish community, *Nature (London)* **554**, 360 (2018).
- [22] L. Pacciani-Mori, S. Suweis, A. Maritan, and A. Giometto, Constrained proteome allocation affects coexistence in models of competitive microbial communities, *ISME J.* **15**, 1458 (2021).
- [23] T. Gibbs, J. Grilli, T. Rogers, and S. Allesina, Effect of population abundances on the stability of large random ecosystems, *Phys. Rev. E* **98**, 022410 (2018).
- [24] J. Grilli, Macroecological laws describe variation and diversity in microbial communities, *Nat. Commun.* **11**, 4743 (2020).
- [25] E. Ser-Giacomi, L. Zinger, S. Malviya, C. De Vargas, E. Karsenti, C. Bowler, and S. De Monte, Ubiquitous abundance distribution of non-dominant Plankton across the global ocean, *Nat. Ecol. Evol.* **2**, 1243 (2018).
- [26] A. Tovo, S. Suweis, M. Formentin, M. Favretti, I. Volkov, J.R. Banavar, S. Azaele, and A. Maritan, Upscaling species richness and abundances in tropical forests, *Sci. Adv.* **3**, e1701438 (2017).
- [27] J. Monod, The growth of bacterial cultures, *Annu. Rev. Microbiol.* **3**, 371 (1949).
- [28] L. Descheemaeker and S. De Buyl, Stochastic logistic models reproduce experimental time series of microbial communities, *eLife* **9**, e55650 (2020).
- [29] E. H. van Nes, D. G. Pujoni, S. A. Shetty, G. Straatsma, W. M. de Vos, and M. Scheffer, A tiny fraction of all species forms most of nature: Rarity as a sticky state, *Proc. Natl. Acad. Sci. U.S.A.* **121**, e2221791120 (2024).
- [30] N. E. Papanikolaou, T. Kypraios, H. Moffat, A. Fantinou, D. P. Perdakis, and C. Drovandi, Predators' functional response: Statistical inference, experimental design, and biological interpretation of the handling time, *Front. Ecol. Evol.* **9**, 749 (2021).
- [31] F. Roy, M. Barbier, G. Biroli, and G. Bunin, Complex interactions can create persistent fluctuations in high-diversity ecosystems, *PLoS Comput. Biol.* **16**, e1007827 (2020).
- [32] T. A. de Pirey and G. Bunin, Many-species ecological fluctuations as a jump process from the brink of extinction, [arXiv:2306.13634](https://arxiv.org/abs/2306.13634).
- [33] See Supplemental Material at <http://link.aps.org/supplemental/10.1103/PhysRevLett.133.167101> for further details and analyses.
- [34] P. Jung and P. Hänggi, Dynamical systems: A unified colored-noise approximation, *Phys. Rev. A* **35**, 4464 (1987). See in particular footnote 14.
- [35] F. Ferraro, C. Grilletta, A. Maritan, S. Suweis, and S. Azaele, Exact solution of dynamical mean-field theory for a linear system with annealed disorder, [arXiv:2405.05183](https://arxiv.org/abs/2405.05183).
- [36] R. Kupferman, G. A. Pavliotis, and A. M. Stuart, Itô versus stratonovich white-noise limits for systems with inertia and colored multiplicative noise, *Phys. Rev. E* **70**, 036120 (2004).
- [37] S. Azaele, S. Pigolotti, J.R. Banavar, and A. Maritan, Dynamical evolution of ecosystems, *Nature (London)* **444**, 926 (2006).
- [38] I. Volkov, J.R. Banavar, S. P. Hubbell, and A. Maritan, Patterns of relative species abundance in rainforests and coral reefs, *Nature (London)* **450**, 45 (2007).
- [39] L. Sidhom and T. Galla, Ecological communities from random generalized Lotka-Volterra dynamics with nonlinear feedback, *Phys. Rev. E* **101**, 032101 (2020).
- [40] J. Hu, D. R. Amor, M. Barbier, G. Bunin, and J. Gore, Emergent phases of ecological diversity and dynamics mapped in microcosms, *Science* **378**, 85 (2022).
- [41] E. Mallmin, A. Traulsen, and S. De Monte, Chaotic turnover of rare and abundant species in a strongly interacting model community, [arXiv:2306.11031](https://arxiv.org/abs/2306.11031).
- [42] L. Poley, J. W. Baron, and T. Galla, Generalized Lotka-Volterra model with hierarchical interactions, *Phys. Rev. E* **107**, 024313 (2023).
- [43] S. Azaele and A. Maritan, Generalized dynamical mean field theory for non-Gaussian interactions, *Phys. Rev. Lett.* **133**, 127401 (2024).